

**ICONE16-48731**

**HIGH-CYCLE THERMAL FATIGUE IN MIXING TEES.  
LARGE-EDDY SIMULATIONS COMPARED TO A NEW VALIDATION EXPERIMENT**

**Johan Westin**

Vattenfall Research and Development AB  
SE-81426 Älvkarleby, Sweden

**Carsten 't Mannetje**

Forsmarks Kraftgrupp AB  
SE-74203 Östhammar, Sweden

**Farid Alavyoon**

Forsmarks Kraftgrupp AB  
SE-74203 Östhammar, Sweden

**Pascal Veber, Lars Andersson**

Onsala Ingenjörbyrå AB  
SE-43437 Kungsbacka, SWEDEN

**Urban Andersson, Jan Eriksson,  
Mats Henriksson**

Vattenfall Research and Development AB  
SE-81426 Älvkarleby, Sweden

**Claes Andersson**

Ringhals AB  
SE-43022 Väröbacka, Sweden

**ABSTRACT**

The present paper describes new experimental data of thermal mixing in a T-junction compared with results from Large-Eddy Simulations (LES) and Detached Eddy Simulations (DES). The experimental setup was designed in order to provide data suitable for validation of CFD-calculations. The data is obtained from temperature measurements with thermocouples located near the pipe wall, velocity measurements with Laser Doppler Velocimetry (LDV) as well as single-point concentration measurements with Laser Induced Fluorescence (LIF).

The LES showed good agreement with the experimental data also when fairly coarse computational meshes were used. However, grid refinement studies revealed a fairly strong sensitivity to the grid resolution, and a simulation using a fine mesh with nearly 10 million cells significantly improved the results in the entire flow domain. The sensitivity to different unsteady inlet boundary conditions was however small, which shows that the strong large-scale instabilities that are present in the mixing region are triggered independent of the applied inlet perturbations.

A shortcoming in the performed simulations is insufficient near-wall resolution, which resulted in poor predictions of the near-wall mean velocity profiles and the wall-shear stress. Simulations using DES improved the near-wall velocity predictions, but failed to predict the temperature fluctuations due to high levels of modeled turbulent viscosity that restrained the formation of small scale turbulence.

**INTRODUCTION**

High-cycle thermal fatigue in the vicinity of T-junctions (mixing Tees) is a potential cause of structural damages, which in some cases have resulted in leaks and power plant shut downs ([1],[2]). Although structural failures can be avoided by installation of static mixers or by regular replacement of components, it is necessary to identify the T-junctions that are at risk. For a detailed structural analysis, both the amplitudes and spectral distribution of the temperature fluctuations near the walls are needed which requires detailed knowledge of the flow field.

The flow in the T-junction is a challenging test case for Computational Fluid Dynamics (CFD), and the CFD-methods based on RANS (Reynolds Averaged Navier-Stokes equations) which are typically used in industrial applications have difficulties to provide accurate results for this flow situation. Recent studies using advanced scale-resolving methods such as LES and DES have shown promising results ([3]-[6]). However, detailed validation of the tools and methods is still required in order to determine their range of validity and their expected accuracy.

The present authors have in a previous study performed experiments and simulations on a T-junction geometry representative for a typical plant installation ([6]). The results were promising but also stressed the need for well-documented experimental data suitable for CFD-validation. The present

paper describes a new experimental and computational effort with the following objectives:

- Provide detailed experimental data on a generic test case of a T-junction suitable for CFD-validation.
- Perform Large-Eddy Simulations with a commercial software (Fluent), with focus on sensitivity studies regarding the influence of mesh resolution and inlet boundary conditions.

### VALIDATION TEST CASE (EXPERIMENTAL DATA)

The model tests were carried out during 2006 at the Älvkarleby Laboratory, Vattenfall Research and Development. The test rig is illustrated in Figure 1, and was designed in order to obtain simple and well-defined inlet boundary conditions. The setup consists of a horizontal pipe with inner diameter 140 mm for the cold water flow ( $Q_2$ ), and a vertically oriented pipe with inner diameter 100 mm for the hot water flow ( $Q_1$ ). The hot water pipe is attached to the upper side of the horizontal cold water pipe. The length of the straight pipes upstream of the T-junction is more than 80 diameters for the cold water inlet, and approximately 20 diameters for the hot water inlet. A stagnation chamber with flow improving devices (tube bundles and perforated plates) is located at the entrance to each of the two inlet pipes. The origin of the coordinate system is in the centre of the T-junction, with the x-, y- and z-directions oriented along the horizontal main pipe, perpendicular to the main pipe and along the branch pipe respectively. The corresponding velocity components are denoted u, v and w.

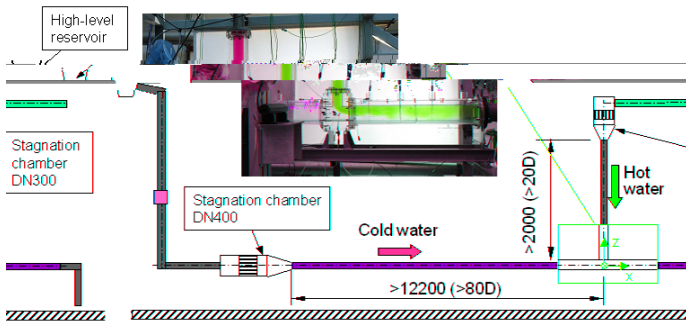


**Figure 1** Side view of the test rig with a photo of the test section. Dimensions are in mm.

The temperature fluctuations near the walls were measured with thermocouples located approximately 1 mm from the pipe wall. Two different types of thermocouples were used, with an estimated frequency response of 30 Hz and 45 Hz respectively. Velocity profiles were measured with two-component Laser Doppler Velocimetry (LDV) in each inlet pipe as well as in cross-sections located 2.6 and 6.6 diameters downstream of the T-junction. The mixing process has also been studied with single-point Laser Induced Fluorescence (LIF) at isothermal conditions. The pipes near the T-junction were made of

plexiglass tubes surrounded by rectangular boxes filled with water in order to reduce the diffraction when the laser beams pass the curved pipe walls.

The tests were carried out with a constant flow ratio  $Q_2/Q_1=2$ , which implies approximately equal flow velocities in the two inlet pipes. The temperature difference between the hot and cold water was  $15^\circ\text{C}$ , and the Reynolds number in both inlet pipes were approximately  $10^5$  for the test case considered in the present paper with bulk velocities of approximately 0.8 m/s. Tests were also carried out with the same flow ratio but varying Reynolds number ( $0.5 \times 10^5$  and  $2 \times 10^5$ ) showing similar results.

As mentioned earlier the aim was to create a generic test case with well-defined inlet boundary conditions. The LDV-measurements in the cold water pipe just upstream of the T-junction showed mean velocity and turbulence profiles in good agreement with experimental data on fully developed pipe flow at similar Reynolds numbers (see e.g. ref. [7]). The length of the hot water inlet pipe was too short (20 diameters) to obtain fully developed flow conditions, but the inlet velocity profiles were measured and used in order to obtain inlet boundary conditions for the simulations.

When comparing computational and experimental results non-dimensional quantities are compared, such as

$$T^* = \frac{T - T_{cold}}{T_{hot} - T_{cold}}$$

$$\frac{T_{rms}}{\Delta T} = \frac{T_{rms}}{T_{hot} - T_{cold}}$$

in which  $\Delta T$  is the temperature difference between the hot and cold water inlets ( $T_{hot} - T_{cold}$ ). The normalization reduces the influence of small temperature variations between different test days. In the results part of the present paper the mean and fluctuating temperatures near the pipe walls are reported at the left, right, top and bottom side of the pipe, which are defined in Figure 2. Due to a mistake when assembling the T-junction, the thermocouples in cross sections  $x=2D$ ,  $4D$ ,  $6D$  and  $8D$  are rotated  $4^\circ$  as compared to the design specifications, which must be taken into account when interpreting the data.

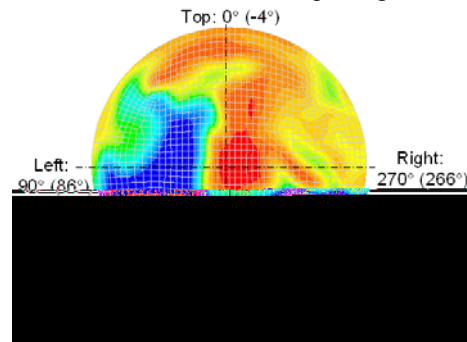


**Figure 2** Illustration of left, right, top and bottom side of the pipe. Cross-section located at  $x=2D$  viewed in the streamwise direction. (Instantaneous temperatures from simulations with mesh 2).

During the course of the study it became clear that it was very difficult to perform laser measurements with temperature differences between the hot and cold water of  $\Delta T \approx 15^\circ\text{C}$ , since the changes in the index of refraction deflected the laser beams. Thus, it was decided that the LDV- and LIF-measurements were carried out at isothermal conditions. The small changes in density and viscosity due to the temperature difference should have a negligible effect on the flow. However, in order to verify this assumption measurements were carried out both at isothermal conditions and with a temperature difference of  $15^\circ\text{C}$  at cross-sections in the hot inlet pipe and downstream of the T-junction at  $x/D=2.6$ . In both cross-sections the isothermal conditions gave almost identical results as obtained with a temperature difference between the two inlet flows.

The uncertainty in the mean temperature measurements with thermocouples is within  $\pm 0.5^\circ\text{C}$ , which gives a constant uncertainty of 0.05 in terms of  $T^*$ . Plots of  $T^*$  and  $Trms$  are based on 45 minutes of data, which gives relatively small statistical uncertainties (typically less than 5% in  $Trms$ , except for a few locations near the bottom wall where the signal is highly intermittent). However, an additional uncertainty of 5% has been added to account for possible systematic errors. The total uncertainty in the temperature fluctuations is estimated to be 10% of the measured value, except near the bottom wall where an uncertainty of 15% has been assumed.

The uncertainty in the LDV-measurements is estimated to be between 6-8% for the different measured quantities, and the estimated uncertainty for the LIF-data is 10%. However, this value only applies to LIF-data that has been corrected for time variations in the inlet concentration.

## COMPUTATIONAL MODEL

### Mesh

Four different meshes have been used in the simulations of the T-junction (see Figure 3). Mesh 1 makes use of four boundary layer cells, and the wall-normal dimension of the first cell is only 0.3 mm in the pipe downstream of the T-junction. Mesh 1B is identical to mesh 1 except that the boundary layer cells are removed. The streamwise resolution is coarsened at a position  $x/D \approx 1.1$ , which can clearly be observed in Figure 3. The total number of cells in mesh 1 and 1B is approximately 0.5 million.

Mesh 2 consists of approximately 1 million cells and has a more uniform cell size distribution throughout the computational domain. This implies that the resolution near the T-junction is similar with mesh 1 and mesh 2, while the streamwise resolution upstream and downstream of the T-junction is higher in mesh 2. No boundary layer cells are used in mesh 2, and the wall-normal dimension of the first cell is approximately 2 mm. Another difference between mesh 1 and mesh 2 is the mesh design in the T-junction. Mesh 1 makes use of an O-type mesh that creates cells with a  $45^\circ$ -skew near the T-junction, while mesh 2 has a different mesh design with less

skewed cells. Mesh 3 is designed similarly as mesh 2 but with a refined grid, resulting in almost 10 million cells.

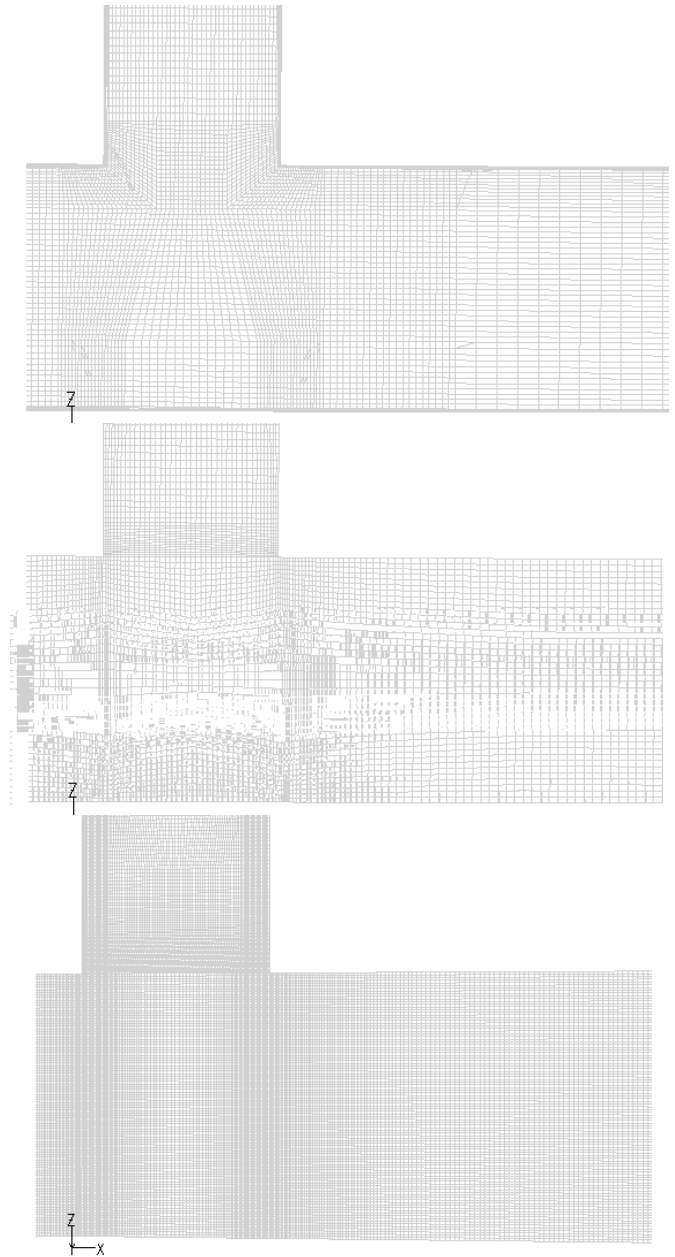


**Figure 3 Mesh 1 (top), mesh 2 (middle) and mesh 3 (bottom). Cross section at  $y=0$ .**

### Numerical schemes

All Large Eddy Simulations reported in the present paper make use of the Wall-Adapting Local Eddy Viscosity (WALE) model. The WALE-model is a Smagorinsky-type model but with a modified dependence on the resolved strain field which is supposed to provide an improved near-wall behavior. Non-iterative time advancement (NITA) has been chosen for time control with a second order implicit scheme. The time step is

set to get a Courant number less than 1 in most of the model, so 1 ms for mesh 1, 0.8 ms for mesh 2 and 0.5 ms for mesh 3 is used. The Fractional Step algorithm has been used for the pressure-velocity coupling. For the pressure, the discretization scheme is Presto, for momentum, Bounded Central Difference and for energy, Quick.

One simulation was also carried out using Detached Eddy Simulations (DES) with the SST  $k-\omega$  model. For more details on the models, see ref. [8].

### Boundary conditions

All calculations make use of adiabatic walls and no-slip boundary conditions. The mean inlet velocity profile for the cold inlet is taken from a RANS-calculation based on a straight pipe with periodical boundary conditions, since the experimental data showed that the flow field is in good agreement with fully developed pipe flow. For the hot inlet, the mean velocity profile is taken from a RANS-calculation under development in order to fit the experimental profile.

Different unsteady inflow boundary conditions have been applied. First of all, simulations were carried out without any unsteady fluctuations applied at the two inlets (“no perturbation”). The second case makes use of the vortex method which is one of the methods implemented in Fluent [8]. A fluctuating (time dependent) vorticity field is added to the mean profiles described in the previous section. The vorticity field is two-dimensional in the plane normal to the streamwise direction, and the spatial distribution and the amplitude of the vortices are governed by the profiles of kinetic energy and dissipation rate obtained from RANS-calculations.

To have better control of the fluctuating velocities at the inlet boundaries a method using isotropic turbulence was applied (see ref. [9] for more details). The isotropic turbulence was scaled and added to the mean velocity profiles obtained from the RANS-calculations, and an instantaneous velocity field was generated for each time step. A file containing 12000 velocity fields (time steps) was generated for each inflow boundary and used as input during the simulation.

### Performed simulations

Table 1 summarizes the main settings in the simulations of the T-junction. The sampling time ( $t_{\text{samp}}$ ) denotes the length of the time sequence used in the data evaluation. Usually the simulation was carried out for approximately 4 seconds before the data sampling was started, which corresponds to at least two complete flow passages through the model.

**Table 1 Performed simulations. All simulations except case T2iso-DES are made with LES using the WALE subgrid-scale model.**

Case	Mesh ID	Mesh #cells	$\Delta t$ (ms)	$Q_2/Q_1$	$t_{\text{samp}}$ (s)	Unsteady BC
T1vm-FKA	1	0.52M	1.0	2.01	29.0	Vortex meth.
T1Bvm	1B	0.45M	-“-	2.01	21.8	-“-
T2vm	2	0.93M	0.8	1.93	19.6	-“-
T2np	2	-“-	-“-	-“-	27.0	No pert.
T2iso	2	-“-	-“-	-“-	13.5	Isotropic turb.
T2iso-DES	2	-“-	-“-	-“-	8.6	Isotropic turb.
T3vm	3	9.5M	0.5	-“-	8.3	Vortex meth.

## RESULTS

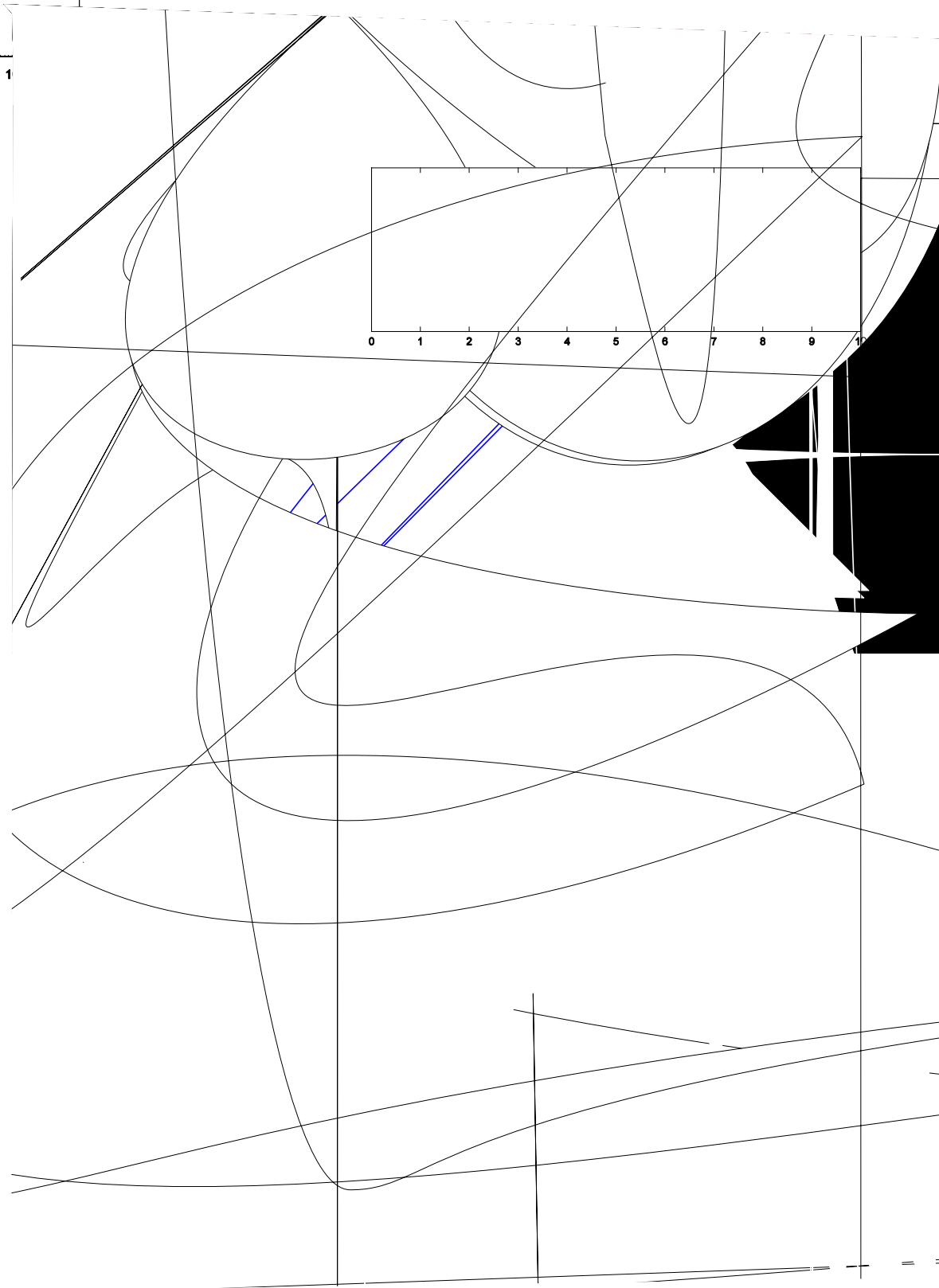
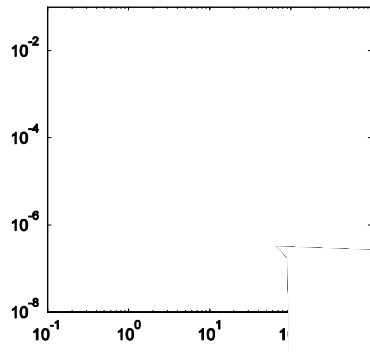
### Temperature data

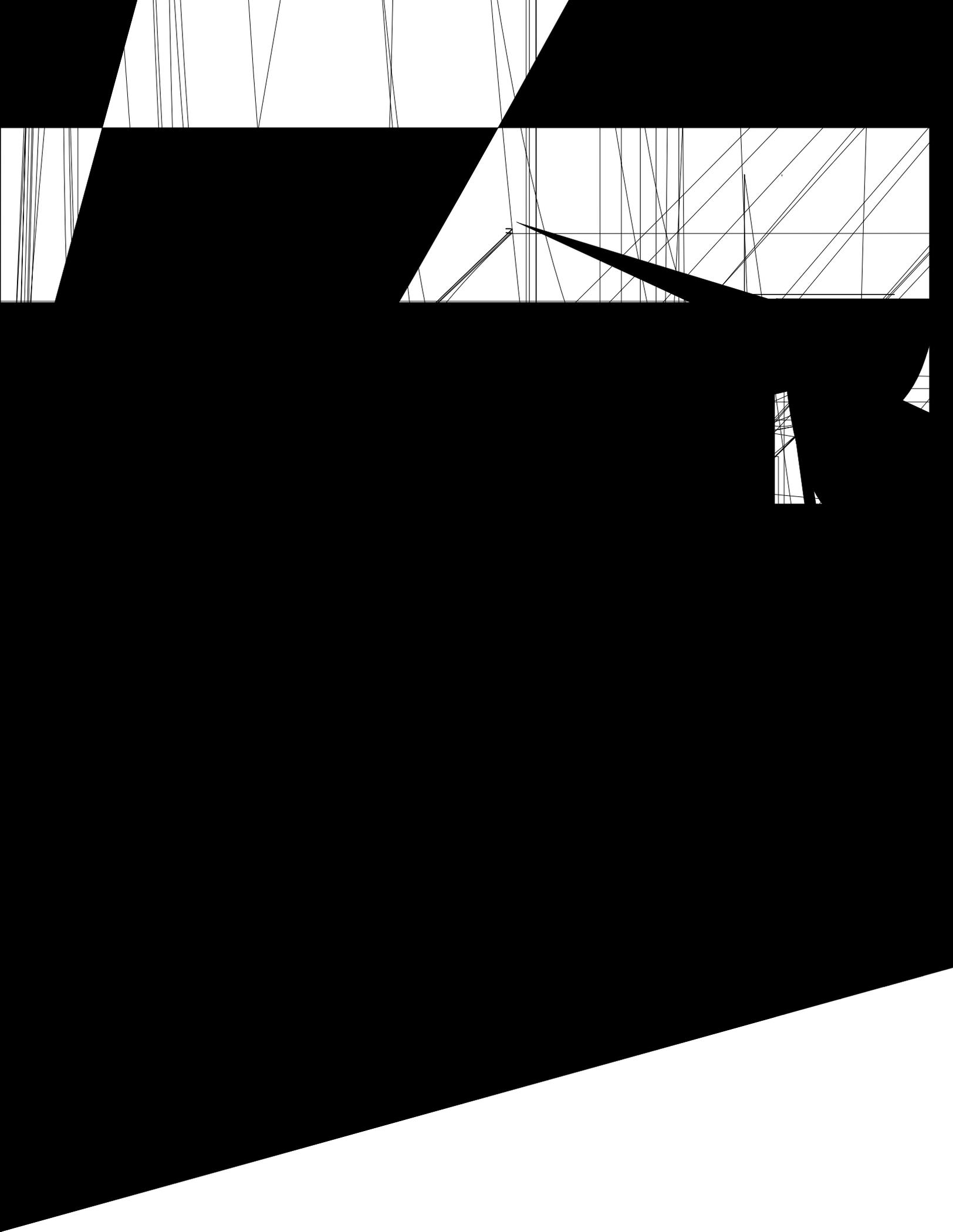
Typical instantaneous temperature fields downstream of the T-junction are illustrated in Figure 4 for simulations with two different mesh resolution. As expected the fine mesh generates more small-scale structures. Quantitative comparisons between experimental data and simulations with different mesh resolution are given in Figure 5 and Figure 6, showing the non-dimensional mean and fluctuating temperatures near the pipe wall at the top, bottom, left and right side of the pipe. The overall agreement between simulations and experiments is good, and considerably better than obtained in refs. [5]-[6] that were based on a previous experimental study. It should also be taken into account that some of the simulation data suffer from a limited sampling time. For example the fluctuations near the bottom wall close to the T-junction originates from a few isolated “spikes” of hot water reaching the bottom wall, and especially for case T3vm the data set is too short to obtain statistically accurate results at this position.

The main discrepancy between simulations and experimental data can be seen in the temperature fluctuations at the left and right side of the pipe at  $x/D=2$ . A significant difference between cases T2vm and T1vm-FKA is that the cell size near the wall is much smaller in the latter case despite the fact that the total number of cells is larger in case T2vm. In case T2vm the wall-normal dimension of the first cell is approximately 2 mm, with only 0.3 mm in case T1vm-FKA. The temperature fluctuations at  $x/D=2$  were considerably smaller in case T1vm-FKA and closer to the experimental data than in case T2vm. When the boundary layer was removed (cf. case T1Bvm), the temperature fluctuations increased close to the values obtained in case T2vm. The best overall agreement, however, was obtained with case T3vm, i.e. the simulation with the finest mesh in the bulk flow. It should be noted that three different subgrid-scale models (WALE, Standard Smagorinsky and Dynamic kinetic energy model) were compared during

Temperature

base case



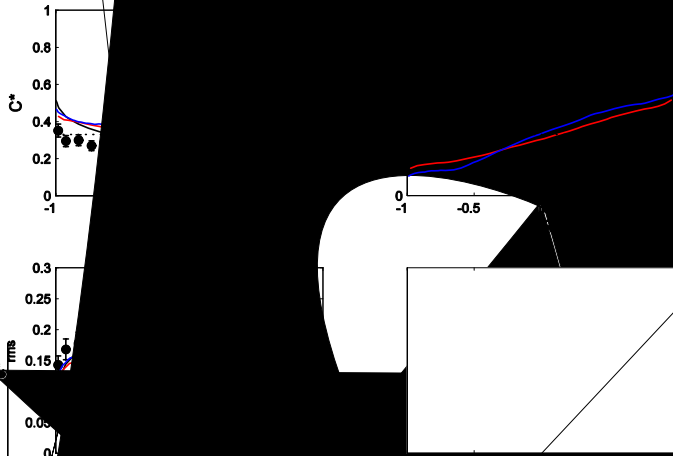




### Concentration

The experim  
measurements w  
(LIF). The mea  
conditions (i.e. e  
pipe), but with a  
Since the temper  
( $\Delta T=15^\circ\text{C}$ ) is s  
between the is  
simulated temper  
dimensional qu  
the simulated  
concentration o

During the  
that a contin  
concentration  
Such correcti  
 $x/D=6.6$  (Fig  
between expe  
fluctuating te  
out at  $x/D=$   
correction w  
data is sign  
discrepancie  
results were





The largest simulation with almost 10 million computational cells gave very good agreement between measured turbulence and temperature fluctuations. However, also in this case the near-wall resolution was insufficient leading to poor predictions of the near-wall mean velocity profiles and the wall-shear stress in the two inlet pipes. The present test case seems to be quite forgiving to this shortcoming and the predicted temperature fluctuations downstream of the T-junction were in good agreement with the experimental data. The difficulty of using LES for wall-bounded flows is well-known and should be kept in mind. It also emphasizes the need for alternative near-wall methods (hybrid methods) in order to use LES as a tool for industrial applications.

## ACKNOWLEDGEMENTS

Fredrik Carlsson and Lars Davidson have provided valuable comments during the course of the present study, and Lars Davidson is also acknowledged for providing data files with isotropic turbulence. The work has been financed by Vattenfall Group functions, Forsmarks Kraftgrupp AB and Ringhals AB.

## REFERENCES

- [1] Faigy, C. (2002) High Cycle Thermal Fatigue: Lessons Learned From Civeaux Event. 2<sup>nd</sup> International Conference on Fatigue of Reactor Components, Snowbird, Utah.
- [2] Chapuliot, S., Gourdin, C., Payen, T., Magnaud, J.P., and Monavon, A. (2005) Hydro-thermal-mechanical analysis of thermal fatigue in a mixing tee, *Nucl. Eng. Des.*, **235**, 575-596.
- [3] Ohtsuka, M., Kawamura, T, Fukuda, T., Moriya, S., Shiina, K., Kurosaki, M., Minami, Y. and Madarame, H. (2003) LES analysis of fluid temperature fluctuations in a mixing Tee pipe with the same diameters, ICONE 11-36064, 11<sup>th</sup> International Conference on Nuclear Engineering, Tokyo, Japan, April 20-23, 2003.
- [4] Braillard, O., Jarny, Y. and Balmigere, G. (2005) Thermal load determination in the mixing Tee impacted by a turbulent flow generated by two fluids at large gap of temperature, ICONE13-50361, 13<sup>th</sup> International Conference on Nuclear Engineering, Beijing, China, May 16-20, 2005.
- [5] Veber, P. and Andersson, L. (2004) CFD calculation of flow and thermal mixing in a T-junction – time dependent calculation – Part 2. Teknisk not 2004/21 Rev 0. Onsala Ingenjörbyrå AB.
- [6] Westin, J., Alavyoon, F., Andersson, L., Veber, P., Henriksson, M. and Andersson, C. (2006) Experiments and unsteady CFD-calculations of thermal mixing in a T-junction, CFD4NRS, Garching, Germany.
- [7] Zagarola, M.V. and Smits, A.J. (1998) Mean-flow scaling of turbulent pipe flow, *J. Fluid Mech.*, **383**, 33-79.
- [8] Fluent version 6.3.26, documentation
- [9] Davidson, L. (2007) Using synthetic fluctuations as inlet boundary conditions for unsteady simulations, *Advances and Applications in Fluid Mechanics*, vol. 1, no. 1, pp. 1-35.